Published in final edited form as:
Cancer Res. 2008 October 1; 68(19): 8039–8048. doi:10.1158/0008-5472.CAN-08-1712.

Addiction to Elevated Insulin-like Growth Factor I Receptor and Initial Modulation of the AKT Pathway Define the Responsiveness of Rhabdomyosarcoma to the Targeting Antibody

Liang Cao[1], **Yunkai Yu**[1,3], **Isaac Darko**[2], **Duane Currier**[2], **Linnia H. Mayeenuddin**[1,3], **Xiaolin Wan**[2], **Chand Khanna**[2], and **Lee J. Helman**[2]

[1]*Genetics Branch, Center for Cancer Research, National Cancer Institute, Bethesda, Maryland* [2]*Pediatric Oncology Branch, Center for Cancer Research, National Cancer Institute, Bethesda, Maryland* [3]*Laboratory of Proteomics and Analytical Technologies, Science Applications International Corporation-Frederick, Inc., National Cancer Institute-Frederick, Frederick, Maryland*

Abstract

Insulin-like growth factor I receptor (IGF-IR) and its ligands are overexpressed by tumors, mediating proliferation and protecting against stress-induced apoptosis. Accordingly, there has been a considerable amount of interest in developing therapeutic agents against IGF-IR. IGF-IR is believed to be ubiquitously expressed without detectable mutation or amplification in cancer. We explored the determinants of cellular response to a humanized anti–IGF-IR antibody. Our results showed a large variation in IGF-IR levels in rhabdomyosarcoma tumor specimens that were comparable with those in rhabdomyosarcoma cell lines. *In vitro* analysis revealed a direct and very significant correlation between elevated IGF-IR levels and antiproliferative effects of the antibody and defined a receptor number that would predict sensitivity. Our data further suggested a strong dependence on IGF-IR for AKT signaling in cells with elevated IGF-IR. The sensitivity of the high IGF-IR–expressing cells was blocked with a constitutively active *AKT*. The extracellular signal-regulated kinase pathway was not affected by the antibody. *In vivo* studies showed that anti–IGF-IR had single-agent antitumor activity; furthermore, predictions of responses based on IGF-IR levels were accurate. *In vivo* biomarker analysis suggested that h7C10 down-regulated both IGF-IR and p-AKT initially, concordant with antitumor activity. Subsequent progression of tumors was associated with reactivation of p-AKT despite sustained suppression of IGF-IR. These results identified the first predictive biomarker for anti–IGF-IR therapies in cancer.

Introduction

Signaling through insulin-like growth factor I receptor (IGF-IR) has been shown to be essential for mammalian growth and development (1,2) and stress response and aging (3). In model systems, numerous studies suggested the roles of IGF-IR in cellular proliferation, stress response and survival, and transformation of normal and tumor cells (4–6). This signaling pathway includes the type I and type II insulin-like growth factors (IGF-I, II) and the common receptor IGF-IR. Some prior studies have shown increased expression of IGF ligands in a

Requests for reprints: Liang Cao, National Cancer Institute, 37 Convent Drive, MSC 4265, Bethesda, MD 20892-4265. Phone: 301-435-9039; Fax: 301-402-3241; E-mail: E-mail: caoli@mail.nih.gov or Chand Khanna, 37 Convent Drive, MSC 4265, Bethesda, MD 20892-4265. Phone: 301-435-9039; Fax: 301-402-3241; E-mail: E-mail: caoli@mail.nih.gov.

Disclosure of Potential Conflicts of Interest
No potential conflicts of interest were disclosed.

variety of cancers and have shown elevated levels of plasma IGF-I associated with increased risk of developing breast, prostate, colorectal, and prostate cancer (4,6–8). IGF-IR is believed to be ubiquitously expressed in normal and cancer tissues (9–11). Many studies show that the activation of IGF-IR results in the induction of two signaling cascades involving AKT and extracellular signal-regulated kinase (ERK; ref. 12). The activation of the AKT pathway is implicated in cell proliferation and survival (4,13), and genes in the AKT pathway are frequently associated with genomic aberrations in a large number of cancers (14,15). Many researchers suggest that IGF-IR can be a rational target for the development of anticancer agents (9,11,16–20).

There are reports of an extensive array of investigational agents against IGF-IR, including small-molecule kinase inhibitors (21–23) and monoclonal antibodies (24–29). NVP-AEW541 and NVP-ADW742 (Novartis) were the first described IGF-IR kinase inhibitors that appeared to have selectivity for IGF-IR in intact cells, despite the lack of selectivity between IGF-IR and IR with *in vitro* inhibitory assays (21,22). These agents inhibited tumor growth in animal models (21–23). Unfortunately, the development of these promising agents has been limited by normal tissue toxicity (30). An antibody targeting the IGF-IR was first reported over 20 years ago using the receptor blocking antibody αIR3 (31). αIR3 was shown to block cell proliferation, survival, and transformation *in vitro* and to have antitumor effects in murine models *in vivo* (32). Recent studies revealed that the ability to down-regulate IGF-IR could be an integral component of the antitumor activity of a number of humanized anti–IGF-IR antibodies (24–29). These antibodies have the promise of greater selectivity over IR and other related receptors. Whereas many of the approved targeted agents work by targeting the "oncogene addiction" of cancer, imatinib works by targeting chronic myelogenous leukemia with *BCR-ABL* translocation or GIST with *c-KIT* mutation, and trastuzumab works by targeting breast cancer with *HER2* amplification, nearly nothing is known about the putative selectivity of anti–IGF-IR based therapies. No specific mutation, translocation, or amplification of *IGF-IR* in cancer has been reported to date. Further, no biomarker has been reported to be associated with response to anti–IGF-IR agents. As some of the anti-IGF-IR–based investigational therapies move into early phases of clinical trials, there is an urgent need to understand the scientific basis for the selective action of these agents. Similarly, it is very important to identify biomarkers that maybe predictive of response so that correlative investigations can be implemented at phase II studies.

Rhabdomyosarcoma is a highly malignant and metastatic pediatric cancer that arises from skeletal muscle and is the most common childhood soft tissue sarcoma that constitutes ~60% of the disease. We previously showed high level of expression of IGF-IR in rhabdomyosarcoma (33) and elevated levels of IGF-II in rhabdomyosarcoma patient samples and cell lines (34). IGF-IR was suggested to be important for the growth of this cancer (35), and a mouse monoclonal antibody against IGF-IR suppressed rhabdomyosarcoma xenograft growth *in vivo* (36). Because IGF-IR is the primary target for all anti–IGF-IR therapies and mutation in *IGF-IR* has not been found in cancers, we reasoned that variations in the levels of IGF-IR may define the degree of dependence of the tumor cells on IGF-IR pathway and therein may predict sensitivity to antibodies that target IGF-IR.

Materials and Methods

Cell lines and reagents

All human rhabdomyosarcoma cell lines, RD, Rh1, Rh4, Rh18, Rh28, Rh30, Rh36, CTR, and RMS13, were maintained in RPMI 1640 with 10% fetal bovine serum (FBS) and antibiotics. Rapamycin was purchased from LC Laboratories; mock antibody MOPC 21 was from Sigma; and anti–IGF-IR h7C10 was kindly provided by Merck. The packaging cell line with a stable constitutively active *AKT* was kindly provided by Dr. Sung-Hyeok Hong. Briefly, a

myristoylated and constitutively active *AKT* was obtained from Upstate. The gene was subsequently cloned into pMSCV and introduced into package cell PT67 according to the protocols from BD Biosciences. The viral supernatant from both the *AKT* and vector cells were used to infect Rh30 cells, followed by puromycin selection to obtain a stable population expressing constitutively active AKT.

Immunoblots and electrochemiluminescence assays

Cells were treated as described and then lysed in RIPA+ buffer complete protease inhibitor cocktail G and phosphatase inhibitor cocktail 1 and 2 (Sigma). Protein concentration of lysates was determined by the BCA protein assay (Pierce). Lysates were separated with Invitrogen NuPage gels and then transferred to nitrocellulose membranes. The blots were probed for the proteins of interest with specific antibodies followed by a secondary antibody (Cell Signaling Technology) and then incubated with SuperSignal chemiluminescence substrate (Pierce). The blots were then exposed to a Kodak Biomax Light Film. The antibodies against ERK, p-ERK (Thr^{202}/Tyr^{204}), AKT and p-AKT (Ser^{473}), p-GSK-3β ($Ser^{21/9}$), and actin were obtained from CST. The antibody against IGF-IR-β (C20) was from Santa Cruz Biotechnology.

The samples used for electrochemiluminescence (ECL) were prepared based on MSD lysate preparation protocol (Meso-Scale Discovery) using complete lysis buffer with protease and phosphatase inhibitors. For quantitative analysis of phospho-AKT and other pathway proteins, the duplex t/p-AKT and duplex t/p-EGFR were obtained from Meso Scale Discovery, used following manufacturer's instructions and read with Sector Imager 2400 (MSD). The antibodies for IGF-IR quantitative immunoassay were purchased from R&D Systems (DuoSet Human Total IGF-IR, DYC305) and adapted to the ECL platform. Briefly, 5 μL/well of 36 μg/mL anti–IGF-IR antibody was coated in coating buffer (0.015% Triton X-100 in PBS) overnight at 4°C. The next day, after blocking with 3% bovine serum albumin (BSA) in blocking buffer [50 mmol/L Tris (pH 7.5), 150 mmol/L NaCl, 0.02% Tween 20], 25 μL cell lysates (1 mg/mL) were added and incubated at room temperature with shaking for 2 h. After washing, 25 μL/well of 400 ng/mL biotin–anti–IGF-IR detection antibody was added, followed by 1 h incubation. For detection, 25 μL/well of 1 μg/mL SULFO-TAG streptavidin (MSD) was added and incubated for 1 h, followed by detection with MSD read buffer. IGF-IR protein amount was determined with a recombinant IGF-IR from R&D Systems (104 kDa excluding glycosylation). EGFR and duplex t/p-AKT assays were performed with MSD kits. Lysates of A431 cells were used as the standard for EGFR quantification at 2 million EGFR per cell.

RNA isolation and quantitative PCR

RNA was prepared with TRIzol per the manufacturer's protocol. mRNA was purified via RNeasy mini spin columns (Qiagen) according to the manufacturer's instructions. The RNA was quantified using a NanoDrop (ND-1000) spectrophotometer.

cDNA was prepared using Superscript III kit (Invitrogen) and quantitative PCR (qPCR) reactions were performed using QuantiTect SYBR Green PCR kit (Qiagen) on a Bio-Rad iCycler. Twenty nanograms of cDNA were used in each 25 μL qPCR reaction. The relative levels of IGF-IR expression were determined using two independent primer sets: IGF-IR F1/R1 GCCAACACTGGTCATCATGGAACT and ATCTTCGGCTACCATGCAATTCCG; IGF-IR F2/R2 ACTATTACCGGAAAGGAGGGAAAGGG and TGTCAGGACAGTTGTCTGGCTTGT. Each primer set was validated and a temperature gradient was performed to establish 60°C as the optimal annealing temperature for PCR amplification. PCR amplification was carried out per the manufacturer's protocols and the C_t values obtained were normalized to β-glucuronidase (β-actin and glyceraldehyde-3-phosphate dehydrogenase were also used as housekeeping controls). The primers for β-

glucuronidase were as follows: HUMGLCB-F1/R1 GAAAATACGTGGTTGGAGAGCTCA and TTGTCTCTGCCGAGTGAAGAT.

Cell viability and clonogenic assays

For ATP-based cell proliferation assay, cells were plated into white 96-well cell culture plates (Nunc) at a density of 2,000 to 10,000 per well for growth inhibition analysis. After 24 h of incubation, drugs were added to the cells in triplicate. At the indicated time, ATPLite assay was performed based on the manufacturer's protocol (Perkin-Elmer) and recorded with a Victor 3 plate reader (Perkin-Elmer). All experiments were performed in triplicate to determine dose responses. At least three repetitive experiments were performed for each cell-drug combination, as well as drug dose studies. For clonogenic assay, 500 cells were plated per well into 6-well plates in triplicates. The following day, h7C10 was added to 10 μg/mL and the cells were incubated further for 2 wk with weekly medium change. The cells were then fixed with 3% glutaraldehyde and stained with 0.5% crystal violet for 30 min. All clonogenic experiments are reproduced.

Human tissues and animal studies

Anonymous human rhabdomyosarcoma tumor and control skeletal muscle tissues were obtained from patients at the National Cancer Institute (NCI). Animal protocol was approved by the NCI Animal Care and Use Committee. Female 4- to 6-wk-old severe combined immunodeficient (SCID) mice were purchased from Charles River Laboratories. Two million rhabdomyosarcoma cells were injected orthotopically into the gastrocnemius muscle of the left hind leg. After 1 wk, mice were randomized to treatment groups of 10 mice: DMSO control, single-agent h7C10, single-agent rapamycin, and h7C10 in combination with rapamycin. The mice were treated with 250 μg h7C10 twice per week, 5 mg/kg rapamycin thrice per week, or 100 μL DMSO diluted to 2% in saline administered i.p. Treatment of all groups was continued until the mice were sacrificed. In the pharmacodynamic experiments, tumor-bearing mice were treated with a single dose of h7C10 by i.p. injection and sacrificed 1, 3, and 5 d after treatment. Four mice were sacrificed at each time point, and four tumor-bearing mice were sacrificed without receiving any h7C10. *In vivo* images were obtained with an imaging system from Xenogen with Rh30-luciferase cells. The diameter was measured twice per week with calipers; when the maximal tumor diameter was measured to be 2 cm, the mice were sacrificed. The tumors were snap frozen and stored at −80°C.

For protein analysis, tissue lysates were made with complete MSD lysis buffer with Matrix D beads (Bio 101) in FastPrep FP120 instrument (Perkin-Elmer) four times (30 s each time at 4° C). Lysates were centrifuged and protein concentration was determined with the BCA kit and normalized for subsequent ECL analysis.

Statistical analyses

Statistical analyses were performed with Prism (GraphPad). Statistical significance was defined as $P < 0.05$. Pearson correlation analysis was performed with Prism.

Results

The growth-inhibitory activity of anti–IGF-IR antibody is highly correlated with the levels of IGF-IR in rhabdomyosarcoma

We screened a group of rhabdomyosarcoma tumors from patients and observed that 5 of 9 tumors had significantly elevated IGF-IR levels when compared with that in normal skeletal muscle using a recombinant IGF-IR as the standard (Fig. 1*A* and *B*). This high and diverse level of expression of IGF-IR (nearly 50-fold) in rhabdomyosarcoma was not expected. A

similar pattern of IGF-IR expression was also seen in rhabdomyosarcoma cell lines (Fig. 1*A*). It is important to note that quantitative assessment of IGF-IR in patient samples and cell lines was performed using a novel sandwich immunoassay (ECL), as it provides the sensitivity (~1 pg), accuracy, reproducibility, and absolute quantification by using a recombinant IGF-IR standard (Fig. 1*B*). The result on IGF-IR quantification from ECL was further validated by qPCR (Fig. 1*C*) and Western blot analysis with a different antibody against IGF-IR (Fig. 1*D*) on selected rhabdomyosarcoma cell lines with high, medium, and low IGF-IR. Strong agreement on both mRNA and protein levels in rhabdomyosarcoma cell lines were seen with all three types of assays. Thus, our results showed a significant variation in IGF-IR in rhabdomyosarcoma cell lines and tumors, and ECL assay on IGF-IR provided specific and accurate quantification of the protein.

We next asked whether the differences in IGF-IR expression in rhabdomyosarcoma cell lines would predict their sensitivity to a humanized antibody h7C10 against IGF-IR. The h7C10 was shown to inhibit IGF-I–mediated activation of IGF-IR and to have single-agent activity in xenograft models (27). Previous studies with humanized anti–IGF-IR antibodies were performed in serum-free conditions or in low-serum conditions with IGF-I supplementation (25,27,28). Given concerns with biological relevance of such conditions, we assessed the effects of h7C10 against rhabdomyosarcoma cell lines grown in 10% FBS. Significant h7C10-mediated growth-inhibitory effects were seen in selected cell lines. Pearson correlation analysis revealed a highly significant correlation between growth-inhibitory effects of h7C10 and the levels of IGF-IR in the rhabdomyosarcoma cell lines (Fig. 2*A*). Rh4 and CTR are the most sensitive cell lines, expressing the highest levels of IGF-IR; RD, Rh30, and RMS13 have medium level IGF-IR and are modestly sensitive; whereas Rh1, Rh18, and Rh36 are resistant to h7C10, expressing the lowest levels of IGF-IR. The h7C10 is extremely potent in inhibiting the proliferation of sensitive Rh4 cells with an IC_{50} of 7 ng/mL or 60 pmol/L; yet, it is inactive with resistant Rh18 cells at 10 μg/mL (Fig. 2*B*), suggesting that the effect is highly specific. The growth-inhibitory effects of the IGF-IR antibody was further validated with clonogenic assay in which h7C10 had minimal effects on low IGF-IR–expressing cells (Rh18), significant inhibition on medium IGF-IR–expressing cells (Rh30), and complete inhibition in cells expressing high IGF-IR (Rh4; Fig. 2*C*). Thus, our results suggest a strong, highly specific, and positive correlation between the level of IGF-IR and *in vitro* anti-proliferative activity of h7C10 in rhabdomyosarcoma cells.

Rhabdomyosarcoma cells with elevated IGF-IR require the receptor for maintaining high steady-state AKT signaling

We next sought to define the mechanisms of the growth-inhibitory response of rhabdomyosarcoma cells to h7C10. We determined the activation status of phospho-AKT (p-AKT) and phospho-ERK (p-ERK) as markers of AKT and mitogen-activated protein kinase pathway activities in these cells in 10% serum. There was close agreement between basal levels of IGF-IR and p-AKT among the cell lines (Fig. 3*A* and *B*). At <3,000 IGF-IR molecules per cell, the AKT pathway is minimally active. EGFR levels were also determined by ECL and calibrated against EGFR in A431 cells (2×10^6 receptors per cell; ref. 37). There was no concordance between IGF-IR and p-ERK (Fig. 3*A* and *B*). Rather, EGFR was better correlated with p-ERK. Thus, IGF-IR levels are specifically correlative with basal p-AKT.

To determine if IGF-IR is required to maintain p-AKT in rhabdomyosarcoma, the cells were treated with the anti–IGF-IR antibody. h7C10 treatment resulted in a rapid decrease in IGF-IR (Fig. 3*C*), likely mediated through receptor internalization (26). Although h7C10 had no detectable effect on p-ERK, it significantly down-regulated p-AKT in cell lines with high IGF-IR in the presence of complete medium (Fig. 3*D*). ECL results further showed a 6-fold reduction of p-AKT in sensitive Rh30 (20K IGF-IR per cell), compared with a 30% reduction of p-AKT

in resistant Rh1 (2.6K IGF-IR per cell) with low steady-state p-AKT (Fig. 3*D*). The activation of the AKT pathway was implicated in cell proliferation and survival (4,13) and associated with genomic aberrations in a large number of cancers (14,15). Our results suggested that IGF-IR was primarily responsible for maintaining high steady-state activation of AKT in rhabdomyosarcoma cells expressing elevated IGF-IR, thus demonstrating a cellular dependence on IGF-IR for AKT signaling.

Constitutively active AKT in part circumvents the growth-inhibitory effect of IGF-IR antibody in sensitive rhabdomyosarcoma cells

To causally link p-AKT pathway with the growth-inhibitory activity of h7C10 in rhabdomyosarcoma cells, we expressed a constitutively active (CA) myristoylated *AKT1* with 1 to 11 amino acids of avian *c-src* at the 5′ end and a 26-amino-acid Myc-His tag at the 3′ end in sensitive Rh30 cells. Western blot indicated the expression of slow migrating CA-AKT protein at a substantially lower level than the endogenous AKT (t-AKT; Fig. 4*A*). The CA-AKT was hyperphosphorylated and appeared to lead to the hypophosphorylation of endogenous AKT (p-AKT; Fig. 4*A*). The expression of CA-AKT rendered the Rh30 cells resistant to h7C10-mediated inhibition of p-AKT and its downstream target p-GSK3β (Fig. 4*A*). When the cells were examined in short-term growth assays, although both cells grew at a similar rate without the antibody, the Rh30-CA-AKT cells were more resistant to h7C10 than Rh30-v-ctrl (Fig. 4*B* and *C*). Long-term clonogenic assay confirmed that CA-AKT resulted in a partial resistance to h7C10 (Fig. 4*D*). In summary, the results suggested that the constitutively active AKT, when expressed at a low level, was able to prevent h7C10-mediated inhibition of AKT signaling and partially rescued the growth-inhibitory effects of h7C10 on rhabdomyosarcoma cells.

In vivo selectivity of antitumor activity for the IGF-IR antibody in rhabdomyosarcoma cells is correlated with elevated IGF-IR

To examine the *in vivo* activity of h7C10, cell line RD was orthotropically injected to the gastrocnemius muscle in SCID mice. After 1 week, groups of 10 mice were treated with placebo or h7C10 continuously with tumors measured twice weekly. The results indicated that h7C10 significantly inhibited RD tumor growth *in vivo* (Fig. 5*A*). A similar antitumor activity was also observed in a second rhabdomyosarcoma xenograft model with the Rh30 cell line (Fig. 6*A* and *B*). As predicted by *in vitro* studies, no significant antitumor effect was seen in low IGF-IR Rh18 cells following h7C10 treatment (Fig. 5*B*). Thus, the data indicate that anti–IGF-IR antibody has selective single-agent antitumor activity against rhabdomyosarcoma cells expressing elevated IGF-IR.

IGF-IR is required for maintaining high AKT signaling *in vivo*

We next conducted biomarker analysis in rhabdomyosarcoma xenografts treated with h7C10. Previous studies showed that IGF-IR antibody treatment resulted in a rapid reduction of IGF-IR (26–29); however, there was no report on the effect on p-AKT with these antibodies *in vivo*. We analyzed IGF-IR and p-AKT in both RD and Rh30 xenografts. The results with RD xenografts showed down-regulation of IGF-IR and an inhibition of p-AKT after 1, 3, and 5 days of h7C10 treatment (Fig. 5*C*), suggesting that the AKT pathway was inhibited with anti–IGF-IR treatment *in vivo*. In comparison, the levels of t-AKT were minimally affected by h7C10 (Fig. 5*C*). Similar reductions of both IGF-IR and p-AKT were reproduced with Rh30 xenograft after 5 days of h7C10 treatment (Fig. 6*C*). Thus, both IGF-IR and p-AKT may be used as pharmacodynamic markers to assess the effects of anti–IGF-IR therapy in rhabdomyosarcoma. More importantly, rhabdomyosarcoma cells with high IGF-IR are addicted to the elevated receptor for maintaining their AKT activation *in vivo* and as such can be effectively modulated with anti–IGF-IR therapy.

Long-term assessment of tumor growth in the xenografts showed that, despite a significant delay in tumor growth with h7C10 treatment, all tumors eventually escaped the inhibition of anti–IGF-IR and grew with similar growth curves as control groups for both RD and Rh30 xenografts (Figs. 5*A* and 6*A*). These parallel rates of tumor growth, following a lag, suggested the acquisition of resistance during continuous h7C10 exposure. We reexamined tumor biomarkers in the escaping rhabdomyosarcoma tumors using tumors collected at the end of the study. In tumors treated with h7C10, there was sustained down-regulation of IGF-IR in RD cells even when RD xenografts were no longer growth inhibited by h7C10 (Fig. 5*D*). In contrast, p-AKT was not inhibited by h7C10, suggesting the uncoupling of IGF-IR down-regulation and p-AKT inhibition in RD xenograft. This finding was again reproduced in Rh30 treated with h7C10 (Fig. 6*D*). Examination of tumor specimens revealed no difference in both total and p-EGFR levels or in the level of PTEN (data not shown) with pretreatment and posttreatment samples. Further studies are needed to define the mechanism of p-AKT reactivation following h7C10 therapy.

Anti–IGF-IR antibody cooperates with rapamycin against rhabdomyosarcoma xenografts

Because the resistance appeared to be associated with reactivation of AKT, we asked whether the combination of h7C10 and rapamycin, which targets the IGF-IR-AKT axis downstream of AKT, would prevent this escape in tumor control. Rapamycin had a very small single-agent effect and minimal combinatory effect with h7C10 on Rh30 xenograft early on (Fig. 6*A* and *B*). However, the combinatory antitumor effect became apparent when the h7C10-treated arm started to grow and the combination resulted in more sustained antitumor effect (Fig. 6*A*). Biomarker analysis of tumors revealed elevated p-AKT in the rapamycin arm; the addition of h7C10 with rapamycin led to reduced p-AKT to a level comparable with that of h7C10 alone (Fig. 6*D*). This result is in agreement with our previous *in vitro* data that rapamycin treatment leads to elevated p-AKT via a putative IGF-IR–dependent pathway (38). Accordingly, the combination of IGF-IR suppression by h7C10 and downstream targeting of mammalian target of rapamycin (mTOR) results in a dual benefit of preventing tumor escape seen after h7C10 treatment alone, presumably by mTOR inhibition downstream of AKT and limiting the potential problem of mTOR-induced up-regulation of AKT.

Discussion

The success of clinical development of molecular targeting agents depends on the identification of susceptible patients in which the targets are absolutely required for tumor pathogenesis and progression. No such information is currently available for anti-IGF-IR–based investigational therapies. In this study, we provide for the first time both *in vitro* and *in vivo* data suggesting that the expression level of IGF-IR in rhabdomyosarcoma cells predicts the response to IGF-IR antibodies: minimal growth inhibition for rhabdomyosarcoma cell lines with <3,000 receptors per cell and maximal inhibition for those with >30,000 receptors per cell. The clinical relevance of these findings is supported by the demonstration of a similar diversity of IGF-IR levels in rhabdomyosarcoma patient tumors. Mechanistic and biomarker studies suggest a cellular addiction in rhabdomyosarcoma cells expressing high IGF-IR, in which 80% to 90% of AKT signaling depends on elevated IGF-IR, both *in vitro* and *in vivo*. Further, AKT pathway modulation is necessary for the activity of anti–IGF-IR, as rhabdomyosarcoma cells expressing constitutively activated AKT are more resistant. The escape from initially effective single-agent IGF-IR therapy in rhabdomyosarcoma xenografts appears to be mediated in part by reactivation of AKT signaling despite sustained suppression of IGF-IR levels during continuous h7C10 therapy. Finally, the late escape from single-agent h7C10 treatment is blocked by the combination therapy of the IGF-IR antibody and the mTOR inhibitor rapamycin. Collectively, our results provide the scientific basis and detection methods to enable clinical correlative studies that may define responders in rhabdomyosarcoma and perhaps a few other

sarcoma patients treated with IGF-IR antibodies; they also provide a framework to consider appropriate drug combinations.

We did not find evidence of ERK pathway inhibition in rhabdomyosarcoma cell lines treated with h7C10. It is important to note that our studies were conducted in the presence of complete medium, without depriving cells of any other growth factor. Previous studies in cancer cells have indicated that IGF-IR could be involved in the activation of ERK pathway and anti–IGF-IR antibodies inhibited IGF-induced activation of p-ERK under conditions of serum starvation (25,28,29). In our studies, the levels of IGF-IR did not correlate with p-ERK. In Rh4 cells where the highest level of IGF-IR was observed, the p-ERK level was rather low. Interestingly, the p-ERK levels were better correlated with that of EGFR, suggesting distinct pathways for activating either AKT or ERK. Based on this, it is reasonable to consider the combination of anti–IGF-IR and anti-EGFR in rhabdomyosarcoma. Recent studies in a lung cancer xenograft model indicated that the combination of anti–IGF-IR and anti-EGFR reduced tumor growth more than either agent alone (27).

Consistent with our *in vitro* results, the *in vivo* pharmacodynamic marker analysis showed that h7C10 was capable of down-regulating IGF-IR and initially inhibiting AKT pathway in cells with elevated IGF-IR. Our data also showed an 8-fold reduction of IGF-IR after 5 days of treatment and 6-fold reduction of IGF-IR at the end of h7C10 treatment in Rh30 tumors, indicating that the effects of the antibody in down-regulating IGF-IR was durable. Similarly, h7C10 led to significant down-regulation of IGF-IR in the RD xenograft model immediately following the initiation of h7C10 treatment and at the end of study. Thus, the anti–IGF-IR antibody leads to the sustained down-regulation of IGF-IR in tumors in both *in vivo* models and the IGF-IR level is a reliable biomarker for exposure to anti–IGF-IR therapy. In comparison, h7C10 resulted in an initial inhibition of p-AKT in both xenograft models, in concordance with the inhibition of tumor growth. The p-AKT levels eventually recovered after tumors resumed growth in the presence of h7C10. There could be many explanations that may account for the uncoupling of IGF-IR–mediated AKT regulation: an alternative receptor, an activating mutation or altered expression of key genes in the AKT pathway, or the removal of a negative regulator of the AKT pathway. Our studies revealed that neither PTEN nor t/p-EGFR levels (not shown) was responsible for this AKT reactivation. Further work is required to understand how rhabdomyosarcoma cells become independent of IGF-IR for AKT signaling.

To begin addressing the problem of single-agent resistance to h7C10 and the uncoupling of IGF-IR inhibition with p-AKT seen in resistant tumors *in vivo*, we considered the opportunity to avert the effects of p-AKT uncoupling by targeting the downstream mTOR. Rapamycin is a highly specific inhibitor of protein kinase target of rapamycin (mTOR), and a rapamycin analogue was recently approved for treating advanced kidney cancer. mTOR regulates protein homeostasis via the ribosomal S6 kinase and the eukaryotic initiation factor 4E-binding protein 1 (39,40). In addition, our previous *in vitro* studies revealed rapamycin-induced feedback activation of AKT in rhabdomyosarcoma cells that was dependent on IGF-IR, and the combination of rapamycin and h7C10 had a small additional benefit *in vitro* (38). In this study, we showed that the combination of IGF-IR and mTOR inhibition provided significant benefit against rhabdomyosarcoma when compared with either agent alone *in vivo*. The analysis of p-AKT in tumors taken from the animals at the end of the study showed that rapamycin induced p-AKT and h7C10 appeared to inhibit such induction, agreeing with our previous cell culture data (38). Rapamycin is a well-tolerated agent and may have potential against a broader range of cancers. Our results suggest that one may achieve improved antitumor activity with the combination of rapamycin and an IGF-IR antibody by targeting two steps of an integrated receptor-AKT-mTOR pathway.

The phosphatidylinositol 3-kinase (PI3K) pathway is one of the most frequently mutated pathways in many cancers where mutations in *PI3KCA*, *PTEN*, and *AKT1* are common (14, 15). By using rhabdomyosarcoma as a model that is largely free from mutation of the above genes, we showed that the antiproliferative effect of an IGF-IR antibody could be partially circumvented with a modest expression of a constitutively active *AKT* gene. Such a finding might suggest that in cancers with activating mutations of the genes in the AKT pathway, the effects of an anti–IGF-IR antibody could be compromised. Thus, it would be useful to carry out mutational analysis of *PI3KCA*, *PTEN*, and *AKT1* in clinical trials with an anti–IGF-IR therapy. Another interesting observation was that the expression of a low level of constitutively active AKT resulted in significant inhibition of the endogenous AKT activity (Fig. 4*A*), giving a constant level of p-AKT, suggesting yet another putative autofeedback regulation of p-AKT. Although much is known about IGF-IR or receptor-mediated AKT activation, there is little information on such feedback regulation. As there are many inhibitors targeting IGF-IR, PI3K, and AKT in early stages of drug development, the understanding of such a feedback regulation could prove to be useful. We are currently pursuing this line of investigation.

In summary, our results point to a cellular dependence of the cancer cells on elevated IGF-IR receptor for activated AKT pathway and cell proliferation in rhabdomyosarcoma. Our results suggest that the elevated levels of IGF-IR may be predictive of anti–IGF-IR response: The antiproliferative and antitumor response was highly correlated with IGF-IR level *in vitro* and *in vivo*; rhabdomyosarcoma with elevated IGF-IR had high p-AKT that was primarily dependent on IGF-IR signaling *in vitro* and *in vivo*; the expression of a constitutively active AKT circumvented the inhibitory effects of anti–IGF-IR; and, whereas the anti–IGF-IR antibody was capable of down-regulating IGF-IR and p-AKT initially *in vivo*, the down-regulation of IGF-IR was uncoupled from inhibiting p-AKT when tumors became resistant to the antibody, which provided a rationale for a combination with rapamycin in producing a lasting therapeutic effect. Our study may provide the scientific basis and the technical know-how for future clinical correlative studies to assess the value of IGF-IR levels as a predictor of response to anti–IGF-IR therapies.

Acknowledgements

Grant support: Intramural Research Program of the NIH, NCI, Center for Cancer Research. This project was also funded in part with federal funds from the NCI, NIH, under contract N01-CO-12400. The content of this publication does not necessarily reflect the views or policies of the Department of Health and Human Services, nor does mention of trade names, commercial products, or organizations imply endorsement by the U.S. Government.

We thank Dr. David Brooks (Merck) for providing us with h7C10 antibody, Dr. Sung-Hyeok Hong (Pediatric Oncology Branch, NCI, Bethesda, MD) for providing the retrovirus packaging cells with myristoylated and constitutively active *AKT*, and Dr. Konrad Huppi (Genetics Branch, NCI, Bethesda, MD) for technical assistance.

References

1. Baker J, Liu JP, Robertson EJ, Efstratiadis A. Role of insulin-like growth factors in embryonic and postnatal growth. Cell 1993;75:73–82. [PubMed: 8402902]
2. Liu JP, Baker J, Perkins AS, Robertson EJ, Efstratiadis A. Mice carrying null mutations of the genes encoding insulin-like growth factor I (Igf-1) and type 1 IGF receptor (Igf1r). Cell 1993;75:59–72. [PubMed: 8402901]
3. Holzenberger M, Dupont J, Ducos B, et al. IGF-1 receptor regulates lifespan and resistance to oxidative stress in mice. Nature 2003;421:182–7. [PubMed: 12483226]
4. Kurmasheva RT, Houghton PJ. IGF-I mediated survival pathways in normal and malignant cells. Biochim Biophys Acta 2006;1766:1–22. [PubMed: 16844299]
5. LeRoith D, Roberts CT Jr. The insulin-like growth factor system and cancer. Cancer Lett 2003;195:127–37. [PubMed: 12767520]

6. Pollak MN, Schernhammer ES, Hankinson SE. Insulin-like growth factors and neoplasia. Nat Rev 2004;4:505–18.
7. Furstenberger G, Senn HJ. Insulin-like growth factors and cancer. Lancet Oncol 2002;3:298–302. [PubMed: 12067807]
8. Renehan AG, Zwahlen M, Minder C, O'Dwyer ST, Shalet SM, Egger M. Insulin-like growth factor (IGF)-I, IGF binding protein-3, and cancer risk: systematic review and meta-regression analysis. Lancet 2004;363:1346–53. [PubMed: 15110491]
9. Tao Y, Pinzi V, Bourhis J, Deutsch E. Mechanisms of disease: signaling of the insulin-like growth factor 1 receptor pathway-therapeutic perspectives in cancer. Nat Clin Pract Oncol 2007;4:591–602. [PubMed: 17898809]
10. Kooijman R. Regulation of apoptosis by insulin-like growth factor (IGF)-I. Cytokine Growth Factor Rev 2006;17:305–23. [PubMed: 16621671]
11. Mitsiades CS, Mitsiades N. Treatment of hematologic malignancies and solid tumors by inhibiting IGF receptor signaling. Expert Rev Anticancer Ther 2005;5:487–99. [PubMed: 16001956]
12. Laviola L, Natalicchio A, Giorgino F. The IGF-I signaling pathway. Curr Pharm Des 2007;13:663–9. [PubMed: 17346182]
13. Manning BD, Cantley LC. AKT/PKB signaling: navigating downstream. Cell 2007;129:1261–74. [PubMed: 17604717]
14. Hennessy BT, Smith DL, Ram PT, Lu Y, Mills GB. Exploiting the PI3K/AKT pathway for cancer drug discovery. Nat Rev Drug Discov 2005;4:988–1004. [PubMed: 16341064]
15. Brugge J, Hung MC, Mills GB. A new mutational AKTivation in the PI3K pathway. Cancer Cell 2007;12:104–7. [PubMed: 17692802]
16. Miller BS, Yee D. Type I insulin-like growth factor receptor as a therapeutic target in cancer. Cancer Res 2005;65:10123–7. [PubMed: 16287993]
17. Baserga R. The insulin-like growth factor-I receptor as a target for cancer therapy. Expert Opin Ther Targets 2005;9:753–68. [PubMed: 16083341]
18. Clemmons DR. Modifying IGF1 activity: an approach to treat endocrine disorders, atherosclerosis and cancer. Nat Rev Drug Discov 2007;6:821–33. [PubMed: 17906644]
19. LeRoith D, Helman L. The new kid on the block(ade) of the IGF-1 receptor. Cancer Cell 2004;5:201–2. [PubMed: 15050909]
20. Sachdev D, Yee D. Inhibitors of insulin-like growth factor signaling: a therapeutic approach for breast cancer. J Mammary Gland Biol Neoplasia 2006;11:27–39. [PubMed: 16947084]
21. Garcia-Echeverria C, Pearson MA, Marti A, et al. *In vivo* antitumor activity of NVP-AEW541—a novel, potent, and selective inhibitor of the IGF-IR kinase. Cancer Cell 2004;5:231–9. [PubMed: 15050915]
22. Mitsiades CS, Mitsiades NS, McMullan CJ, et al. Inhibition of the insulin-like growth factor receptor-1 tyrosine kinase activity as a therapeutic strategy for multiple myeloma, other hematologic malignancies, and solid tumors. Cancer Cell 2004;5:221–30. [PubMed: 15050914]
23. Scotlandi K, Manara MC, Nicoletti G, et al. Antitumor activity of the insulin-like growth factor-I receptor kinase inhibitor NVP-AEW541 in musculoskeletal tumors. Cancer Res 2005;65:3868–76. [PubMed: 15867386]
24. Sachdev D, Li SL, Hartell JS, Fujita-Yamaguchi Y, Miller JS, Yee D. A chimeric humanized single-chain antibody against the type I insulin-like growth factor (IGF) receptor renders breast cancer cells refractory to the mitogenic effects of IGF-I. Cancer Res 2003;63:627–35. [PubMed: 12566306]
25. Burtrum D, Zhu Z, Lu D, et al. A fully human monoclonal antibody to the insulin-like growth factor I receptor blocks ligand-dependent signaling and inhibits human tumor growth *in vivo*. Cancer Res 2003;63:8912–21. [PubMed: 14695208]
26. Cohen BD, Baker DA, Soderstrom C, et al. Combination therapy enhances the inhibition of tumor growth with the fully human anti-type 1 insulin-like growth factor receptor monoclonal antibody CP-751,871. Clin Cancer Res 2005;11:2063–73. [PubMed: 15756033]
27. Goetsch L, Gonzalez A, Leger O, et al. A recombinant humanized anti-insulin-like growth factor receptor type I antibody (h7C10) enhances the antitumor activity of vinorelbine and anti-epidermal growth factor receptor therapy against human cancer xenografts. Int J Cancer 2005;113:316–28. [PubMed: 15386423]

28. Wang Y, Hailey J, Williams D, et al. Inhibition of insulin-like growth factor-I receptor (IGF-IR) signaling and tumor cell growth by a fully human neutralizing anti-IGF-IR antibody. Mol Cancer Ther 2005;4:1214–21. [PubMed: 16093437]
29. Wu JD, Odman A, Higgins LM, et al. *In vivo* effects of the human type I insulin-like growth factor receptor antibody A12 on androgen-dependent and androgen-independent xenograft human prostate tumors. Clin Cancer Res 2005;11:3065–74. [PubMed: 15837762]
30. Garber K. IGF-1: old growth factor shines as new drug target. J Natl Cancer Inst 2005;97:790–2. [PubMed: 15928295]
31. Arteaga CL, Osborne CK. Growth inhibition of human breast cancer cells *in vitro* with an antibody against the type I somatomedin receptor. Cancer Res 1989;49:6237–41. [PubMed: 2553250]
32. Arteaga CL, Kitten LJ, Coronado EB, et al. Blockade of the type I somatomedin receptor inhibits growth of human breast cancer cells in athymic mice. J Clin Invest 1989;84:1418–23. [PubMed: 2553774]
33. El-Badry OM, Minniti C, Kohn EC, Houghton PJ, Daughaday WH, Helman LJ. Insulin-like growth factor II acts as an autocrine growth and motility factor in human rhabdomyosarcoma tumors. Cell Growth Differ 1990;1:325–31. [PubMed: 2177632]
34. Wan X, Helman LJ. Levels of PTEN protein modulate Akt phosphorylation on serine 473, but not on threonine 308, in IGF-II-overexpressing rhabdomyosarcomas cells. Oncogene 2003;22:8205–11. [PubMed: 14603261]
35. Shapiro DN, Jones BG, Shapiro LH, Dias P, Houghton PJ. Antisense-mediated reduction in insulin-like growth factor-I receptor expression suppresses the malignant phenotype of a human alveolar rhabdomyosarcoma. J Clin Invest 1994;94:1235–42. [PubMed: 8083365]
36. Kalebic T, Tsokos M, Helman LJ. *In vivo* treatment with antibody against IGF-1 receptor suppresses growth of human rhabdomyosarcoma and down-regulates p34cdc2. Cancer Res 1994;54:5531–4. [PubMed: 7923191]
37. Wiley HS. Anomalous binding of epidermal growth factor to A431 cells is due to the effect of high receptor densities and a saturable endocytic system. J Cell Biol 1988;107:801–10. [PubMed: 3262110]
38. Wan X, Harkavy B, Shen N, Grohar P, Helman LJ. Rapamycin induces feedback activation of Akt signaling through an IGF-1R-dependent mechanism. Oncogene 2007;26:1932–40. [PubMed: 17001314]
39. Bjornsti MA, Houghton PJ. Lost in translation: dysregulation of cap-dependent translation and cancer. Cancer Cell 2004;5:519–23. [PubMed: 15193254]
40. Bjornsti MA, Houghton PJ. The TOR pathway: a target for cancer therapy. Nat Rev 2004;4:335–48.

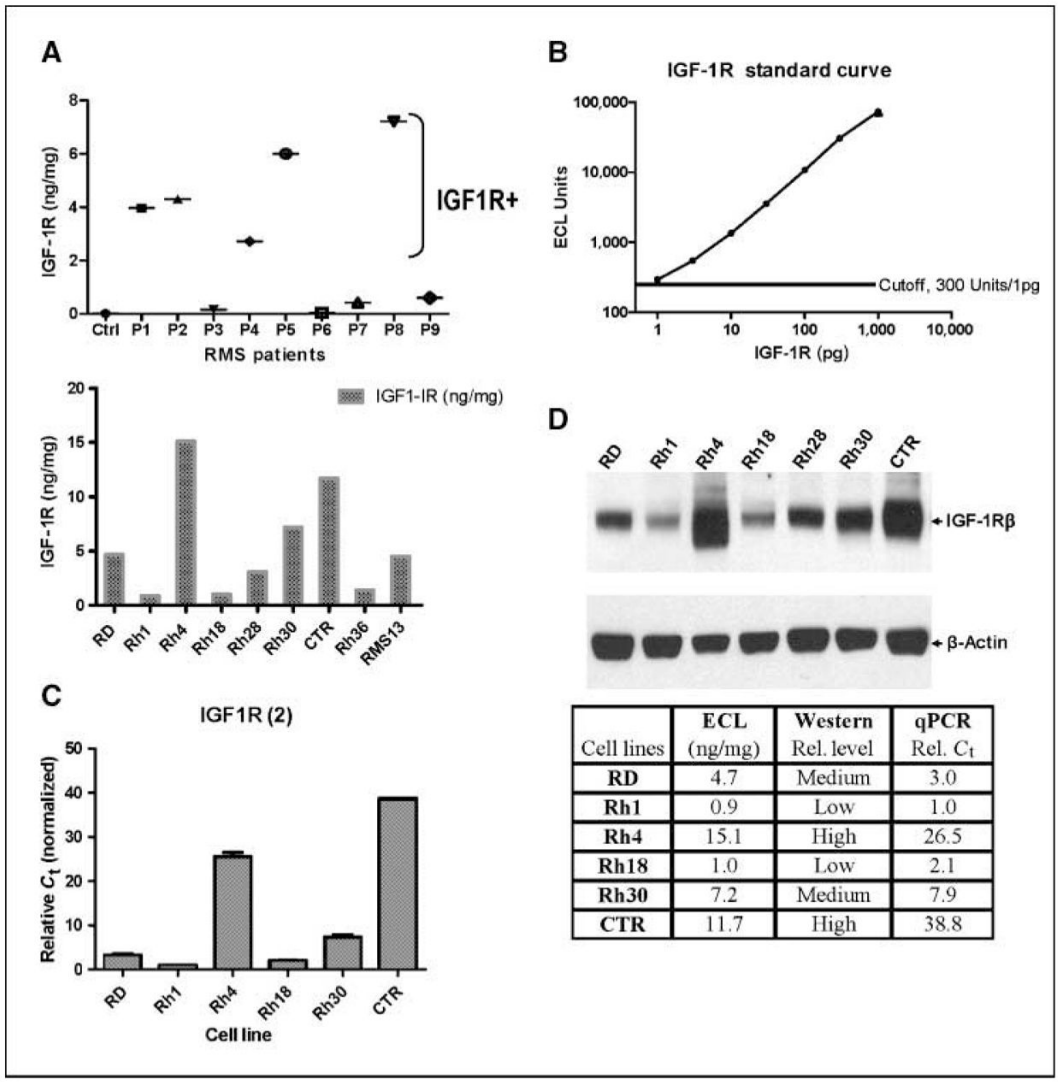

Cell lines	ECL (ng/mg)	Western Rel. level	qPCR Rel. C_t
RD	4.7	Medium	3.0
Rh1	0.9	Low	1.0
Rh4	15.1	High	26.5
Rh18	1.0	Low	2.1
Rh30	7.2	Medium	7.9
CTR	11.7	High	38.8

Figure 1.

Determination of IGF-IR in rhabdomyosarcoma tumors and cell lines and validation of ECL-based IGF-IR sandwich immunoassay assay. *A*, levels of IGF-IR in rhabdomyosarcoma (*RMS*) tumors and cell lines. IGF-IR was determined for tumor tissue from rhabdomyosarcoma patients. *Ctrl*, skeletal muscle from a donor; *P1-P9*, rhabdomyosarcoma tumors from patients at the NCI. IGF-IR was also determined for a panel of rhabdomyosarcoma cell lines. Data are shown as nanograms of IGF-IR per milligram of lysate. *B*, standard curve was generated with purified recombinant IGF-IR with ECL assay (see Materials and Methods). *Points*, mean (n = 3), with coefficient of variation of ~10%; *bars*, SE. Cutoff was defined from negative controls (1% BSA) as mean + 5 × SD. The assay has a sensitivity of 1 pg IGF-IR. *C*, IGF-IR mRNA in rhabdomyosarcoma cell lines was determined with normalized qPCR analysis. *D*, IGF-IR protein was detected with immunoblot with a different IGF-IR antibody. The results of IGF-IR mRNA and protein analysis were summarized to show high degrees of agreement between ECL, immunoblot, and qPCR results.

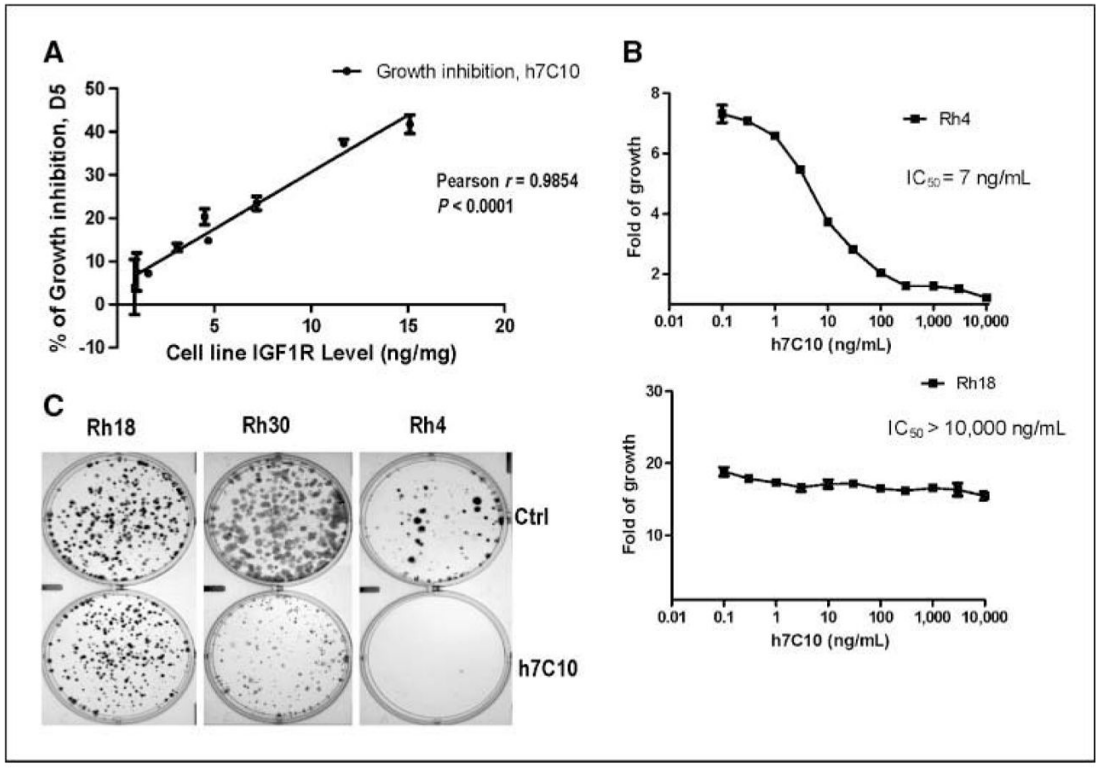

Figure 2.

In vitro antiproliferative activity of h7C10 is correlated with the levels of IGF-IR in rhabdomyosarcoma cells *A*, rhabdomyosarcoma cell lines were treated with 10 μg/mL anti–IGF-IR antibody h7C10 or a mock antibody (MOPC 21) for 5 d. The cell proliferation was determined using ATP assay. The percentage of inhibition was defined as $(V_{ctrl} - V_{treated})/V_{ctrl}$. The data were obtained from a representative proliferation experiment and analyzed against their IGF-IR levels using GraphPad. *Points*, mean ($n = 3$); *bars*, SE. Pearson correlation was performed with GraphPad to determine the correlation between antiproliferative activity of h7C10 and IGF-IR levels of the rhabdomyosarcoma cell lines. *B*, dose curve of h7C10 in antiproliferative assay against sensitive Rh4 (IC_{50}, 7 ng/mL) and resistant Rh18 cells (IC_{50} >10,000 ng/mL). *Points*, mean ($n = 3$); *bars*, SE. *C*, effects of h7C10 on rhabdomyosarcoma in clonogenic assay with representative rhabdomyosarcoma cell lines of low (Rh18, 1.0 ng/mg), medium (Rh30, 7.2 ng/mg), and high (Rh4, 15.1 ng/mg) levels of IGF-IR.

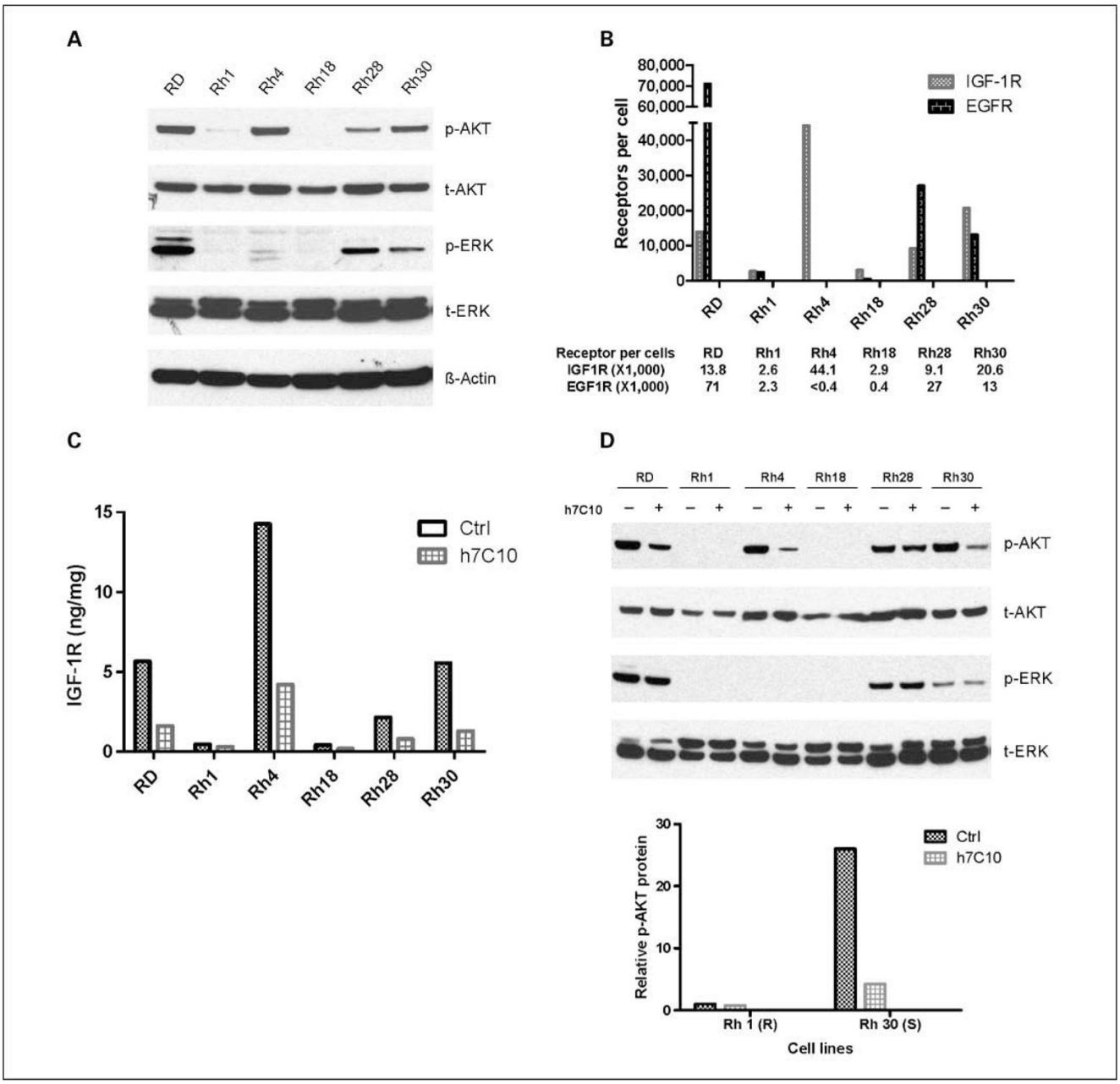

Figure 3.

Correlation between IGF-IR and p-AKT levels in rhabdomyosarcoma cell lines and a cellular dependence on IGF-IR for endogenous AKT signaling in the presence of 10% serum. *A*, immunoblot analysis of AKT, p-AKT, ERK, and p-ERK in rhabdomyosarcoma cell lines. *B*, quantitative analysis of EGFR and IGF-IR in the rhabdomyosarcoma cell lines. The number of EGFR molecules per cell was determined in reference to that in A431 at 2×10^6 EGFR per cell. The number of IGF-IR molecules per cell was determined with a recombinant IGF-IR standard. *C*, down-regulation of IGF-IR by h7C10. Rhabdomyosarcoma cell lines were treated with 10 μg/mL anti–IGF-IR antibody h7C10 for 24 h. The cell lysates were analyzed for total IGF-IR via an ECL immunoassay. *D*, the cell lysates from *C* were analyzed with immunoblots against t/p-EKR and t/p-AKT. Further quantitative ECL analysis of p-AKT following h7C10

treatment was performed and the relative levels of p-AKT were shown in a bar chart. Resistant Rh1 cells: ctrl, 1; h7C10, 0.75. Sensitive Rh30 cells: ctrl, 26; Rh30, 4.2.

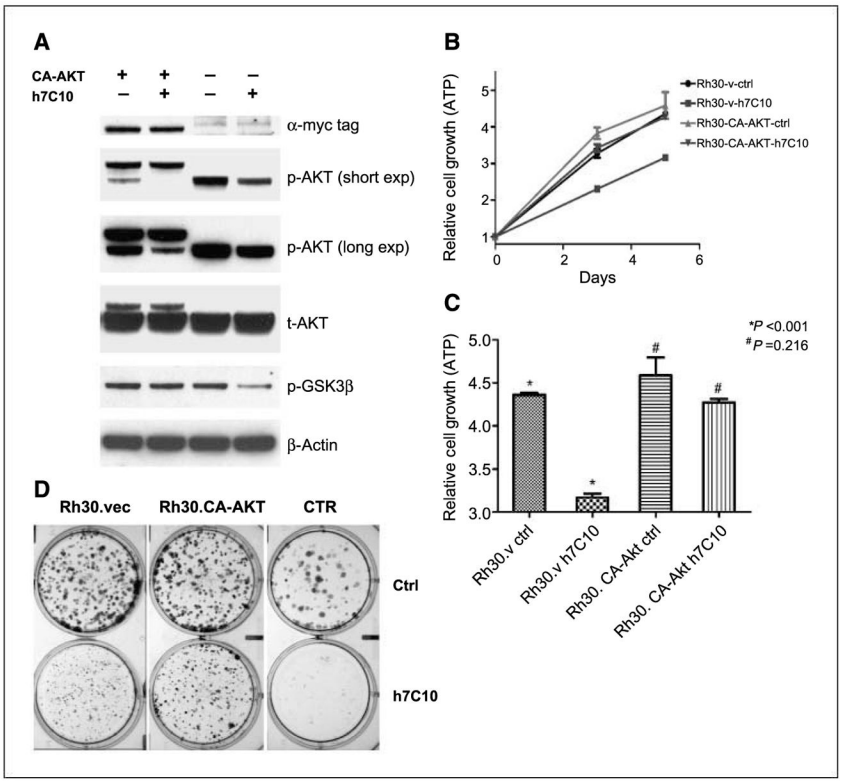

Figure 4.

Evaluation of the role of AKT pathway in h7C10-mediated growth suppression with a constitutively active (*CA*) *AKT* gene. *A*, immunoblot analysis of Rh30-v and Rh30-CA-AKT cells treated with anti–IGF-IR antibody h7C10. Cells were infected with retroviruses containing the vector or *CA-AKT* gene, selected with puromycin, and pooled. The stable cells were treated with h7C10 for 24 h and analyzed for myc-tag, total and p-AKT, and a downstream target p-GSK3β. CA-AKT migrates at a slower rate when compared with the endogenous AKT. *B*, examination of the antiproliferative activity of h7C10 in Rh30-CA-AKT cells. Cells infected with vector and CA-AKT viruses were treated with mock or h7C10 for 3 and 5 d. The results are from a representative experiment. *Points*, mean ($n = 3$); *bars*, SE. *C*, statistical analysis of Rh30.v and Rh30-CA-Akt cells treated with h7C10 for 5 d, followed by ATP measurement in triplicate. *Columns*, mean ($n = 3$); *bars*, SE. Student's *t* test was performed and *P* values of relevant pairs are shown. *D*, effects of h7C10 on Rh30-vec and Rh30-CA-AKT in a clonogenic assay. CTR is another rhabdomyosarcoma cell line with very high IGF-IR level and is very sensitive to h7C10. Cells were treated with h7C10 in triplicates for 2 wk before fixing and staining.

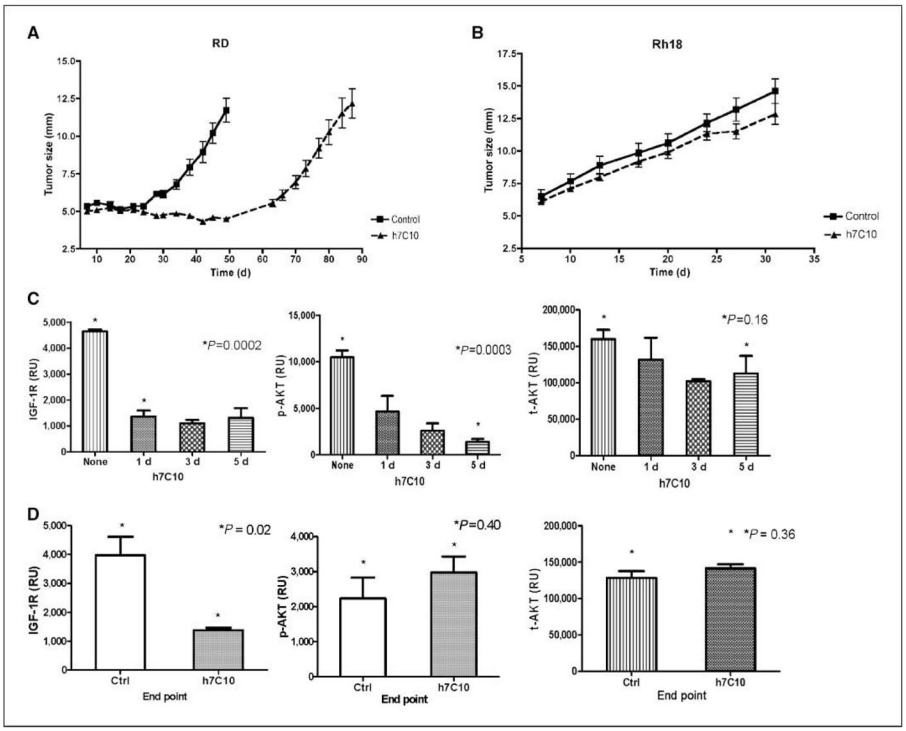

Figure 5.

In vivo antitumor effects of h7C10 against rhabdomyosarcoma and biomarker analysis*A*, mice with RD xenografts were treated with saline or h7C10 starting from day 8. Data shown represent the average size of the tumor in their maximal diameter. *Points*, mean (n = 10); *bars*, SE. *B*, mice with Rh18 xenografts (low IGF-IR) were treated with saline or h7C10 from day 8. *Columns*, mean maximal diameter (n = 10); *bars*, SE. *C*, pharmacodynamic marker analysis of IGF-IR, p-AKT, and t-AKT following 1 to 5 d of h7C10 treatment with RD xenografts (n = 3). *D*, end point analysis of IGF-IR, p-AKT, and t-AKT with RD tumors collected at the end of the experiment (n = 4). *Columns*, mean relative ECL units; *bars*, SE. *P* values for relevant pairs are shown.

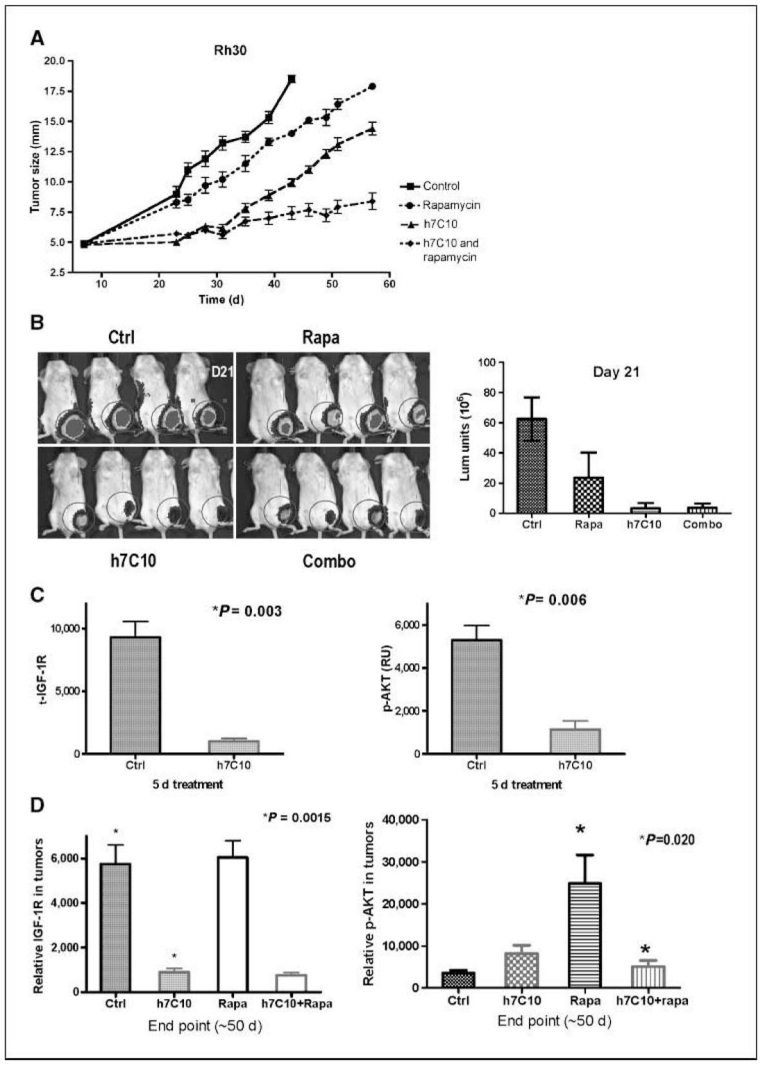

Figure 6.

In vivo antitumor effects of h7C10 and rapamycin*A*, a four-arm study with h7C10 and rapamycin against mice with rhabdomyosarcoma cell line Rh30. Mice were treated with DMSO, h7C10, rapamycin, or both from day 8. *Points*, mean maximal diameter (n = 10); *bars*, SE. *B*, after 2 wk of drug treatment, *in vivo* tumor imaging was performed with a Xenogen imager. *Columns*, mean luminescence units (n = 4); *bars*, SE. *C*, PD marker analysis of IGF-IR and p-AKT following 5 d of h7C10 treatment (n = 3). *D*, end point analysis of IGF-IR and p-AKT with tumors collected at the end of the experiment (n = 4). *Columns*, mean relative ECL units; *bars*, SE. *P* values for the relevant pairs are shown.